https://doi.org/10.5194/angeo-2019-123
Preprint. Discussion started: 27 August 2019

Annales Geophysicae Discussions
Open Access
EGU

Characterization of gravity waves in the lower ionosphere using VLF observations at Comandante Ferraz Brazilian Antarctic Station

Emilia Correia[1,2], Luis Tiago Medeiros Raunheitte[2], José Valentin Bageston[3], Dino Enrico D´Amico[2]

[1]Instituto Nacional de Pesquisas Espaciais, INPE, São José dos Campos-SP, Brazil
[2]Centro de Rádio Astronomia e Astrofísica Mackenzie, Universidade Presbiteriana Mackenzie, São Paulo-SP, Brazil
[3]Centro Regional Sul de Pesquisas Espaciais, CRS/INPE, Santa Maria-RS, Brazil

Correspondence to: Emilia Correia (ecorreia@craam.mackenzie.br)

https://doi.org/10.5194/angeo-2019-123
Preprint. Discussion started: 27 August 2019

Annales Geophysicae Discussions

Abstract. The goal of this work is to investigate the gravity waves (GWs) characteristics in the low ionosphere using very low frequency (VLF) radio signals. The spatial modulations produced by the GWs affect the conditions of the electron density at reflection height of the VLF signals, which produce fluctuations of the electrical conductivity in the D-region that can be detected as variations in the amplitude and phase of VLF narrowband signals. The analysis considered the VLF signal transmitted from the US Cutler/Marine (NAA) station that was received at Comandante Ferraz Brazilian Antarctic Station (EACF, 62.1^o S, 58.4^o W), which is a great circle path crossing longitudinally the Drake Passage. The wave periods of the GWs detected in the low ionosphere are obtained using the wavelet analysis applied to the VLF amplitude. The use of the VLF technique was validated comparing the wave period and duration properties of one GW event observed simultaneously with a co-located airglow all-sky imager both operating at EACF. The statistical analysis of the wave periods detected using VLF technique for 2007 showed that the GW events occur almost all nights, with a higher frequency per month from March to October. The predominant wave periods are more frequent between 10 and 15 min occurring preferentially during the equinoxes, but there are some events with periods higher than 60 min appearing only in the solstices (January and July). These results show that VLF technique is a powerful tool to obtain the wave period and duration of GW events in the low ionosphere, with the advantage to be independent of sky conditions, and can be used during daytime and year-round.

Keywords: gravity waves, ionosphere, VLF, wavelet, Antarctica

1 Introduction

The upper part of the middle atmosphere, the upper Mesosphere and Lower Thermosphere (MLT), is dominated by the effects of the atmospheric waves (gravity waves, tides and planetary waves) originated at tropospheric and stratospheric layers or even in situ generation. In the last decades, due to the recognized importance of the gravity waves (GW) in the general circulation, structure and variability in the MLT, and as an essential component in the Earth climate system (Fritts and Alexander, 2003; Alexander et al., 2010), these waves had been intensively investigated. For example, Earn et al. (2011) using data from SABER instrument onboard TIMED satellite, estimated the horizontal gravity wave momentum flux and showed that the fluxes at stratospheric heights (40 km) are stronger at latitudes above 50^o in local winter and near the subtropics in the summer hemisphere, which are in agreement with Wang et al. (2005) and Zhang et al. (2012) that used temperature soundings of the same instrument and shows high gravity wave activity over regions of strong convection located at lower latitudes in summer and over the southern Andes and Antarctica Peninsula in winter. The sources of mesospheric GW obtained through high-resolution general circulation model also shows that the dominant sources are steep mountains and strong upper-tropospheric westerly jets in winter and intense subtropical monsoon convection in summer (Sato et al., 2009). Thus, any major disturbances that occur in the stratosphere can significantly modify the GW fluxes, which in turns change the thermal and winds structures of the MLT region. One of these disturbances are the sudden stratospheric warmings (e.g. Schoeberl, 1978), which are large-scale perturbation of the polar winter stratosphere where the gradients of winds and temperatures are reversed for periods of days to weeks.

https://doi.org/10.5194/angeo-2019-123
Preprint. Discussion started: 27 August 2019

The atmospheric gravity waves are originated in the lower atmosphere and propagate upwards, travelling through regions with decreasing density, which results in an exponential grow of their amplitudes (e.g. Andrews et al. 1987). The large wave amplitudes lead to wave breaking that deposits the momentum flux at the MLT region, which comes mostly from waves with periods lower than 30 min (Fritts and Vincent, 1987; Vincent, 2015). Theoretical, numerical and observational studies have improving the understanding of the GW sources, observed parameters (wavelength, period and velocity), propagation directions (isotropic/anisotropic), spectrum of intrinsic wavelengths and periods, and moment fluxes, as well as their impact in the MLT region. A variety of techniques has been used to obtain wave parameters, such as the horizontal and vertical wavelengths, phase speeds and periods, involving satellite observations as well as ground-based instrumentation. Each technique has its own strengths and limitations as presented, for example, by Vincent (2015).

The GW activity has been extensively observed mainly by using airglow all-sky imagers that permit to obtain the horizontal wave parameters and the propagation directions of the small-scale waves (e. g. Taylor et al., 1995). In airglow imagers the GWs are seen as intensity variations of the optical emission from airglow layers located at the MLT region (80 - 100 km altitude), but this technique requires dark and cloud-free conditions during the night, and particularly at high latitudes it is impossible to observe the nightglow during the summer since there are no totally dark condition during this season.

In order to avoid the limitations of the optical airglow observations, other techniques using radio soundings started to be used to characterize the mesospheric GWs in the ionospheric D- and E-regions. The propagation of GWs through the mesosphere induces spatial modulations in the neutral density, which modulates the electron production rate and the effective collision frequency between the neutrals components and electrons in the lower ionosphere. The ionospheric absorption of the cosmic radio noise is a function of the product of these two parameters, and so the fluctuations produced by the effect of GWs can be detected by imaging riometers. The ionospheric absorption modulations observed with different riometer beams permit to infer the gravity wave parameters such as the phase velocity, period and direction of propagation, as demonstrated by Jarvis et al. (2003) and Moffat-Griffin et al. (2008). They validated this technique comparing mesospheric GW signatures observed by using both co-located imaging riometer and airglow imager.

The atmospheric gravity waves also can be detected in lower ionosphere using very low frequency (VLF: 3-30 kHz) radio signals. The amplitude and phase of VLF signals propagating in the Earth-ionosphere waveguide are affected by the conditions of the local electron density at reflection height, which is in the ionospheric D-region. The spatial modulations produced by the GWs in the neutral density produce fluctuations of the electrical conductivity in the D-region, which are detected as variations in the amplitude and phase of VLF narrowband (NB) signals. Acoustic-gravity waves have been detected as amplitude variations of VLF signals associated with solar terminator motions (Nina and Cadez, 2013), with the passage of tropical cyclones crossing the transmitter-receiver VLF propagation path (Rozhnoi et al., 2014), and particularly during nighttime, in association with local convective and lightning activity (Marshall and Snively, 2014). Planetary wave signatures also have been detected in the VLF NB

https://doi.org/10.5194/angeo-2019-123
Preprint. Discussion started: 27 August 2019

Annales Geophysicae Discussions

amplitude data, which effects are pronounced during wintertime and present a predominant quasi 16-day oscillation (Correia et al., 2011, 2013; Schmitter, 2012; Pal et al., 2015).

The advantage of usage radio techniques to observe GWs instead of the optical ones is that they are able to provide observations independently of the sky conditions, even during the daytime, and year-round. The purpose of this paper is to presents the characterization of the GW events detected in the lower ionosphere from the analysis of the VLF NB amplitude of signals detected at Comandante Ferraz Brazilian Antarctic Station (EACF). The GW parameters such as the wave period and the time duration of the GW activity will be obtained from the spectral analysis of the VLF NB amplitude fluctuations. The methodology is validated comparing the derived parameters of GW events using VLF technique with the respective ones detected with a co-located airglow all-sky imager.

2 Instrumentation and data analysis

The VLF signals propagate over long distances inside the Earth-ground cavity, with considerably low attenuation, and are detected by VLF receivers after being reflected in the lower ionosphere at ~70-90 km of height (e.g., Wait and Spies, 1964). The changes detected in the amplitude and phase of the VLF NB signals give information of the D-region physical and dynamic conditions along the transmitter-receiver Great Circle Path (GCP), which are associated with the ionosphere electrical conductivity. This analysis uses VLF signals transmitted from the US Navy stations at Cutler/Maine (24.0 kHz, NAA) and at Lualualei/Hawaii (21.4 kHz, NPM), which after propagating along the GCPs NAA-EACF and NPM-EACF were detected with 1 sec time resolution using a AWESOME receiver (Scherrer et al. 2008) operating at EACF (62.1^{o} S, 58.4^{o} W) station located on King George Island in the Antarctic Peninsula (Fig. 1). The simultaneous study of the VLF signals propagating over these two different paths gives the opportunity to identify the propagation direction of GWs since the transmitters are about 100^{o} apart in longitude.

The GW parameters were obtained from the VLF NB amplitude signals using a wavelet spectral analysis, which gives the wave period and time duration of GW activity, as will be described in the following section. To demonstrate the potentiality of usage of the VLF technique to observe GWs, the spectral analysis is applied during the night of June 10, 2007, when a prominent GW event (mesospheric front) occurred and it was well observed and characterized by using a co-located airglow imager along with temperature profiles form TIMED/SABER and horizontal winds from a medium frequency (MF) radar operated at Rothera station (Bageston et al., 2011). Afterwards, a year-round climatology of GWs of parameters related to the wave periods was obtained from the amplitude data of VLF signals propagating in the NAA-EACF GCP for the full year of 2007.

2.1 Wavelet spectral analysis

The Wavelet analysis was used to obtain the parameters of VLF amplitude signal fluctuations, which might be associated with the time and duration of the GW event and the period range it covers. It is used the tool developed by Torrence and Compo (1998) and including the rectification of the bias in favor of large scales in the wavelet power spectrum, which was introduced by Liu et al. (2007). The analysis uses the Morlet mother wavelet with frequency parameter equal 6, significance level of 95 % and time lag of

https://doi.org/10.5194/angeo-2019-123
Preprint. Discussion started: 27 August 2019

Annales Geophysicae Discussions
Open Access
EGU

0.72 (Torrence and Compo, 1998). The wavelet analysis returns the following general results: the Power Spectrum; the Global Wavelet Spectra, which measures the time-averaged wavelet power spectra over a certain period and its significance level; and scale-averaged wavelet power, that is the weighted sum of the wavelet power spectrum over 2 to 64 band.

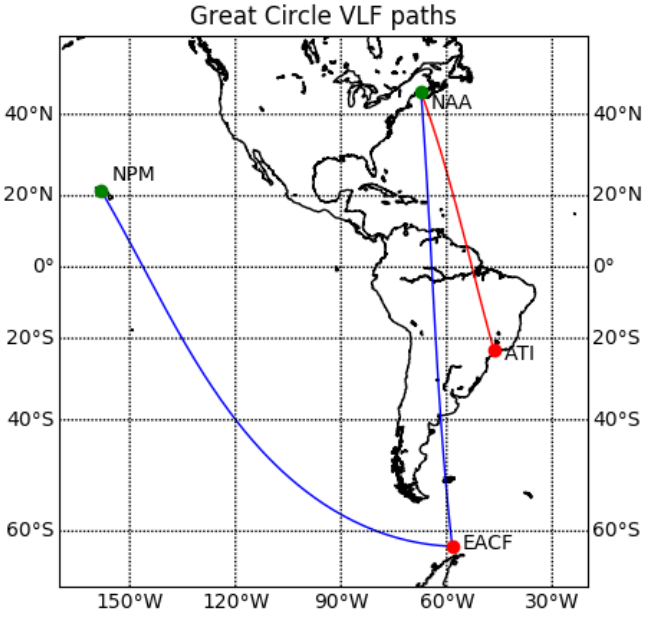

Figure 1: VLF propagation paths from NAA and NPM transmitters to the receiver stations located at Comandante Ferraz Brazilian Antarctic Station (EACF) (blue paths) and Atibaia, São Paulo (red path).

The wavelet analysis was applied to the VLF data obtained at EACF during the night of June 10, 2007, when a GW event was observed with a co-located airglow imager. This was done to compare the wave period and event duration parameters obtained from VLF data with the ones obtained from all-sky images. Figure 2 shows the airglow images of the GW event, which was identified as a mesospheric front (Bageston et al., 2011). The first view of the frontal event observed at EACF was clearly seen in the airglow image obtained at 23:20 LT (LT=UT-3) with a second crest also visible behind the main front, and it was in the field of view up to 23:53 LT. Bageston et al. (2011) reported the analysis from 23:20 to 23:42 LT when it was visible an increase in the number of wave crests (see Fig. 2), inferred as a growth rate of 4 waves h^{-1} in this packet wave during their propagation across the field-of-view of the all-sky imager. The FFT-2D spectral analysis was applied to six images from 23:32 to 23:38 LT on 9 July (2:32 to 2:38 UT on 10 July), and it was obtained the following wave parameters: horizontal wavelength of 33 km, observed period of 6 min and observed phase speed of 92 m s^{-1}. During the same night this event was observed with a co-located near zenithal (field of view about 22° off-zenith) temperature airglow imaging

https://doi.org/10.5194/angeo-2019-123
Preprint. Discussion started: 27 August 2019

Annales Geophysicae Discussions
Open Access
EGU

spectrometer, which observes the OH (6-2) band emission (FotAntar-3, Bageston et al., 2007). The spectral analysis of the temperature showed evidence of gravity waves of small scale with predominant period of ~14 min (Bageston et al., 2011). Since the spectrometer has a smaller field-of-view (~70 km in diameter) compared to the all-sky imager (~300 km of diameter in the un-warped images), the larger predominant periodicity obtained from the temperature could be one component of the main wave observed with airglow all-sky imager. These parameters are similar to the ones obtained for mesospheric fronts or bore-type events, which were understood as a rare type of gravity waves at polar latitudes and was first observed at Halley Station on May 2001 (Nielsen et al., 2006). Nowadays, with more observations, it is clear that the mesospheric fronts or bores are more likely to be observed from middle to high latitude (even at unexpected places as the South Pole) as can be noted in the recent studies on this subject (e.g.: Pautet et al., 2018a, Giongo et al, 2018 and Hozumi et al., 2018).

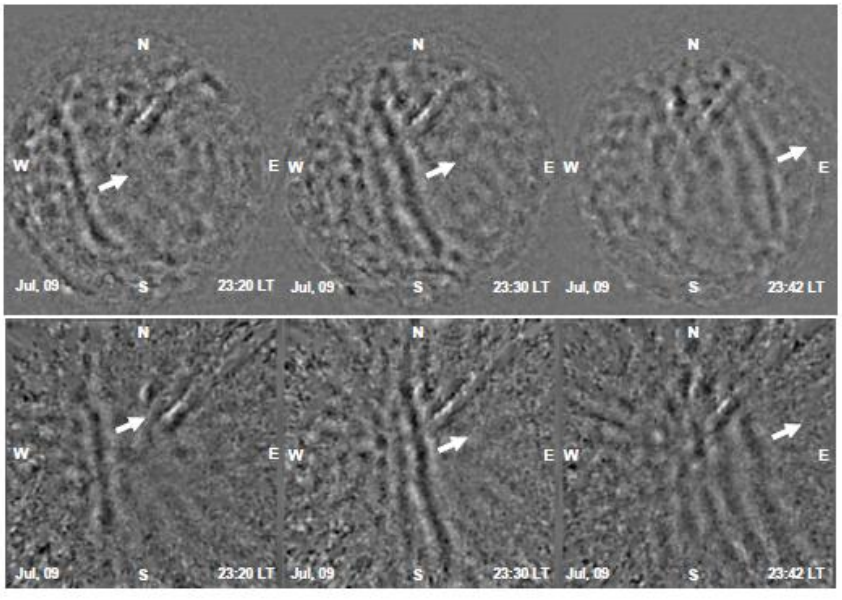

Figure 2: Processed all-sky images of the GW event observed at EACF at three times separated by 10 min on the night of 9-10 July 2007 showing the mesospheric front propagating from southwest to northeast. The first row shows the images with the star field subtracted and applying the Time Difference (TD) image processing, and at the second row are the same images after correcting for the fish-eye lens format. (from Bageston et al., 2011).

The VLF amplitude from NAA transmitter detected at EACF for July 10, 2007 is shown in Fig. 3, where the vertical lines identify the sunrise and sunset hours at the transmitter (SR-T and SS-T, full lines) and receiver (SR-R and SS-R, dashed lines) stations. The wavelet spectral analysis (Fig. 4) was applied to the VLF data from 01:00 to 04:30 UT (22:00 LT June 9 to 01:30 LT on June 10, box in Fig. 3), which covers the nighttime interval of the images obtained with the co-located all-sky imager.

https://doi.org/10.5194/angeo-2019-123
Preprint. Discussion started: 27 August 2019

Figure 4 shows the spectral analysis applied to the VLF amplitude data. The analysis is applied to the residual value obtained after subtracting the raw data from a 10-min running mean (Fig. 4a), in order to characterize the small-scale waves. Figure 4a shows clearly 4 stronger fluctuations in the VLF amplitude between 1:50 and 2:40 UT (22:50 and 23:40 LT), which occurred in close temporal association with the crests identified in the airglow images. The last VLF fluctuation was the strongest one and finished at ~02:40 UT (23:40 LT), near the time when the wave packet started to dissipate as observed in the airglow images (Bageston et al., 2011). The power spectrum of the residual VLF amplitude (Fig. 4b) shows strong significant components with periods between 4 and 16 min, with stronger peaks at ~6 min and 14 min. The global wavelet spectrum (Fig. 4c) shows a stronger component with period between 4 and 8 min that is due six significant events of ~20 min duration (Fig. 4d), with one of them occurring from 2:32 to 2:38 UT (23:32 to 23:38 LT) that is the same time interval the wave period of 6 min was identified in the airglow images. The other significant component with peak at ~14 min is present from 01:50 to 02:40 UT (Fig. 4d), the same time interval when the 4 crests of the mesospheric front were identified in the airglow images, and occurred in close temporal association with the identification of gravity waves with the same period in the spectral analysis of the OH temperature obtained with the co-located imaging spectrometer (Bageston et al., 2011).

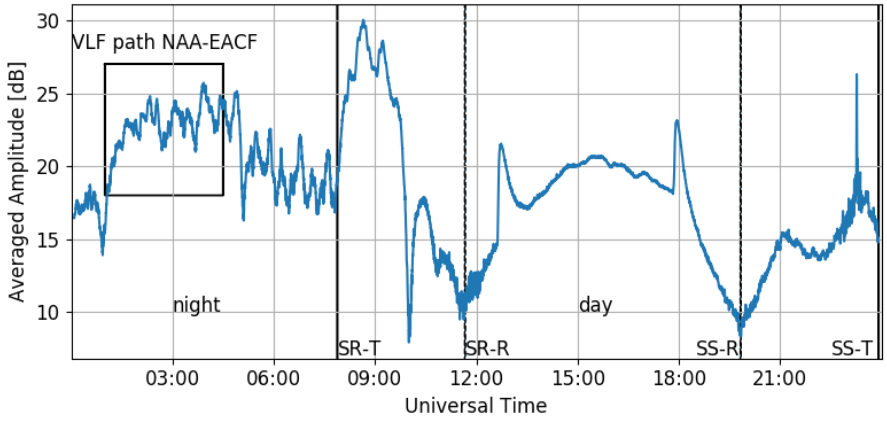

Figure 3: VLF amplitude from NAA transmitter station detected with 15 seconds time resolution at EACF on July 10, 2007. The vertical lines mark the sunrise (SR) and sunset (SS) at NAA transmitter station (T, full lines) and at receiver station (R, dashed lines). The periods of completely night and day in the NAA-EACF VLF path are identified. The box marks the time interval of data used to perform the spectral analysis.

Since the VLF path is long, one test was done to be sure that the wave event is the one detected near EACF and not at any other location in the path between transmitter and receiver. This test considers the wavelet analysis applied to the VLF path NAA-Atibaia (NAA-ATI), which is almost the same trajectory of NAA-EACF but its length is ~50 % shorter. Figure 5 shows no wave events at the time the event detected in the NAA-EACF path, that had association with the GW seen in the airglow imager,

https://doi.org/10.5194/angeo-2019-123
Preprint. Discussion started: 27 August 2019

Annales Geophysicae Discussions
Open Access
EGU

evidencing they occurred in the part of the VLF trajectory closer the EACF station. This test confirms the GW events detected by VLF technique in the NAA-EACF path occurred near Antarctic Peninsula and could be associated with the events observed by the airglow imager operating at EACF.

The characterization of the GWs using VLF amplitude data using wavelet analysis demonstrated the viability to use VLF signals to obtain the period and time duration of the GW events. The use of VLF observations to characterize the GW events permit to obtain their climatology all over years since they do not are affected by the atmospheric conditions and also can be done during daytime.

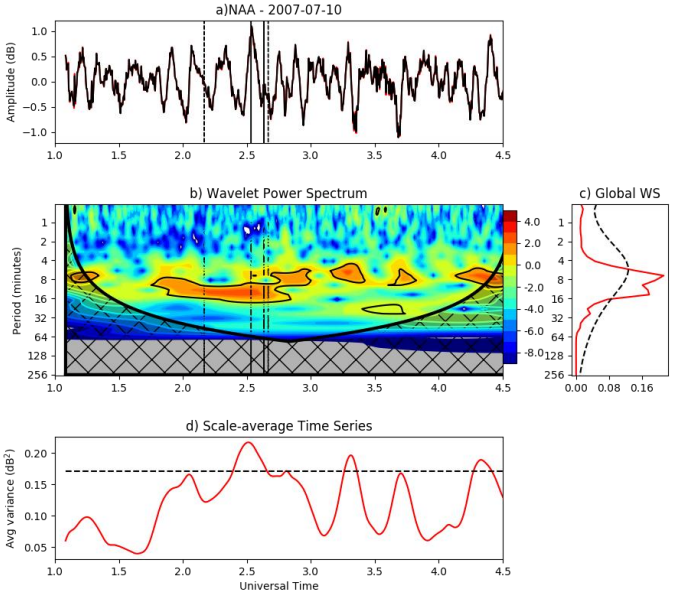

Figure 4: Example of wavelet spectral analysis applied to the VLF amplitude signal in the NAA-EACF GCP on 10 June 2007. (a) The residual VLF amplitude after subtracting the raw data from a10-min running mean. (b) Wavelet power spectra in logarithm (base 2), with regions of confidence levels greater than 95 % (showed with black contours), and the cross-hatched areas indicating the regions where edge effects become important. (c) time-averaged wavelet power spectra (Global WS). (d) scale-averaged wavelet power.

https://doi.org/10.5194/angeo-2019-123
Preprint. Discussion started: 27 August 2019

Annales Geophysicae Discussions
Open Access
EGU

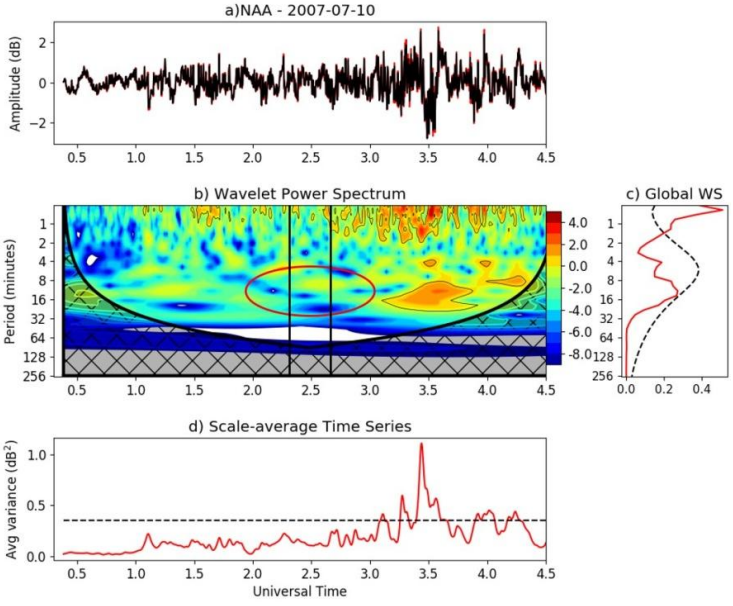

Figure 5: Same as Fig. 4, but for the VLF signal propagating in the NAA-Atibaia VLF GCP.

2.2 Climatology of GW period from VLF signal

The GW climatology is done based on the wavelet analysis applied to the VLF amplitude signal detected during nighttime hours in the NAA-EACF GCP for the full 2007 year. The idea is to compare the wave period year-round climatology obtained with VLF technique with the one obtained with airglow data. The wave period from VLF technique is the predominant component with the highest intensity in the global wavelet power. For example, in the analysis done in the previous sub-section, the predominant wave period is 6 min.

3 Observational results

Here is presented the statistical analysis of the predominant wave period of the GW events detected in the low ionosphere as amplitude fluctuations of the VLF signals received at EACF during 2007, which is compared with the wave period distribution obtained from the events observed with a co-located airglow all-sky imager.

The wave periods in the low ionosphere were analyzed only during night hours in order to compare the results with the wave period obtained using the co-located all-sky imager. Figure 6 shows the number of days of observation per month and respective number of nights with wave events detected in the low ionosphere. The predominant wave periods observed in the low ionosphere were between 5 and 35 min (98 % of the observed days) with only few days (2 %) with periods above 35 min, which were distributed in 5 period ranges from 5 to >35 min (5-10, 10-15, 15-25, 25-35 and >35 min). The GW events were observed almost all nights of the year, but with higher percentage of occurrence per month from March to

https://doi.org/10.5194/angeo-2019-123
Preprint. Discussion started: 27 August 2019

Annales Geophysicae Discussions
Open Access
EGU

October (>80 %), reaching 100 % on September when GW events were observed all nights of this month. This distribution is in agreement with the statistical results of the GW events observed with a co-located airglow all-sky imager, which showed the majority of the waves (~85 %) were observed between June and September (Bageston et al., 2009). The distribution of predominant wave periods by month shows waves with periods >25 min occurred on January and July, during the solstices, while the waves with predominant period in the 5-10 min range occurred preferentially on March-April and August suggesting an equinoctial distribution.

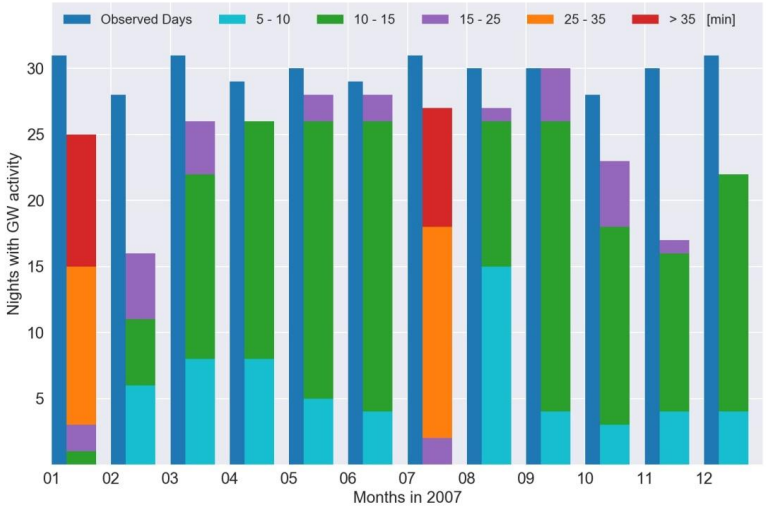

Figure 6: Monthly gravity wave activity at EACF as detected in the low ionosphere using VLF technique during 2007. The dark blue narrow bar shows the number of the observed days per month, and the colored bars show the number of nights per month with GW events observed according to the GWs predominant periods. The bar colors give the number of waves with predominant period observed in each month separated as the following period intervals: 5-10 min (blue), 10-15 min (green), 15-25 min (purple), 25-35 min (orange) and above 35 min (red).

Figure 7 shows the histogram with the distribution of the predominant wave period for the 295 days that have GW events detected in the low ionosphere using the VLF technique. The predominant wave periods were mostly distributed between 5 and 20 min (~ 80 %), with a higher number of occurrences between 10 and 15 min (~50 %), but also presents events with wave period higher than 60 min (~2 %). This wave period distribution is in good agreement with the statistics reported by Bageston et al. (2009) from the analysis of 234 GWs observed with a co-located airglow all-sky imager from April to October 2007.

https://doi.org/10.5194/angeo-2019-123
Preprint. Discussion started: 27 August 2019

Annales Geophysicae Discussions
Open Access
EGU

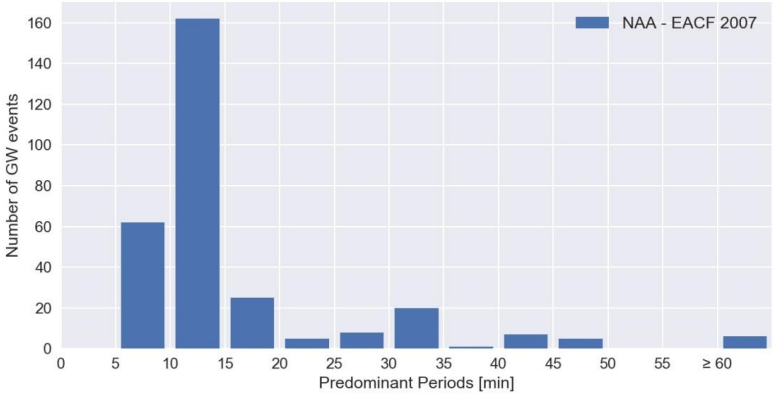

Figure 7: Histogram plot of the predominant observed wave periods of the GWs detected in the low ionosphere as amplitude variations of the VLF signal propagating in the NAA-EACF GCP.

4 Summary

Here we presented an investigation of the GWs characteristics in the low ionosphere, where they produce density fluctuations that were detected as amplitude variations of VLF signals. The analysis used the VLF signal transmitted from the US Cutler/Marine (NAA) station that was received at Comandante Ferraz Brazilian Antarctic Station (EACF), which is a great circle path crossing longitudinally the Drake Passage. The wavelet analysis of the VLF amplitude considered the predominant wave periods observed during night hours to compare with the wave periods obtained from a co-located airglow all-sky imager. The use of the VLF technique was validated comparing the wave period and duration properties of one GW event observed simultaneously with a co-located airglow all-sky imager.

The statistical analysis of the wave period of the GW events detected at EACF using VLF technique for 2007 showed that the GW events were observed almost all nights of the year, but with higher frequency (larger activity) per month from March to October. The predominant wave periods distribution showed that the GWs with periods between 10 and 15 min occurred in higher number when compared to other period bins, but also there were events with periods higher than 60 min. Both results are in good agreement with the wave period distribution of the GW events observed during 2007 with the co-located airglow all-sky imager.

These results show that VLF technique is a powerful tool to obtain the wave period and duration of GW events in the low ionosphere, with the advantage to be independent of sky conditions, and can be used during daytime and year-round. The simultaneously analysis of VLF signals from two distinct transmitter stations apart ~100^{o} in longitude, for example NAA-EACF and NPM-EACF could be used to obtain information about the GWs velocity and direction of propagation.

Competing interests. The authors declare that they have no conflict of interest.

https://doi.org/10.5194/angeo-2019-123
Preprint. Discussion started: 27 August 2019

Acknowledgments. EC thanks National Council for Research and Development - CNPq (processes no: 556872/2009-6, 406690/2013-8 and 306142/2013-9), São Paulo Research Foundation – FAPESP (process no: 2019/05455-2) for individual research support, and the National Institute for Space Research (INPE/MCTI). The authors also acknowledge the support of the Brazilian Ministries of Science, Technology and Innovation (MCTI), of Environment (MMA) and Inter-Ministry Commission for Sea Resources (CIRM). LTMR thanks Coordenação de Aperfeiçoamento de Pessoal de Nível Superior - Brasil (CAPES) - Finance Code 001.

References

Alexander, M. J., Geller, M., McLandress, C., Polavarapu, S., Preusse, P., Sassi, F., Sato, K., Ern, M., Hertzog, A., Kawatani, Y., Pulido, M., Shaw, T., Sigmond, M., Vincent, R., and Watanabe, S.: Recent developments in gravity wave effects in climate models and the global distribution of gravity wave momentum flux from observations and models, Q. J. R. Meteorol. Soc., 136, 1103–1124, https://doi.org/10.1002/qj.637, 2010.

Andrews, D. G., Holton, J. R., and Leovy, C. B.: Middle atmosphere dynamics, Academic Press, London, 1987.

Bageston, J. V., Gobbi, D., Tahakashi, H., and Wrasse, C. M.: Development of Airglow OH Temperature Imager for Mesospheric Study, Revista Brasileira de Geofísica, 25 (Suppl. 2), 27-34, https://dx.doi.org/10.1590/S0102-261X2007000600004, 2007.

Bageston, J. V., Wrasse, C. M., Gobbi, D., Takahashi, H., and Souza, P. B.: Observation of mesospheric gravity waves at Comandante Ferraz Antarctica Station (62 S), Ann. Geophys., 27, 2593–2598, https://doi.org/10.5194/angeo-27-2593-2009, 2009.

Bageston, J. V., Wrasse, C. M., Batista, P. P., Hibbins, R. E., Fritts, D. C., Gobbi, D., and Andrioli, V. F.: Observation of a mesospheric front in a thermal-doppler duct over King George Island, Antarctica, Atmos. Chem. Phys., 11, 12137–12147, https://doi.org/10.5194/acp-11-12137-2011, 2011.

Correia, E., Kaufmann, P., Raulin, J.-P., Bertoni, F., and. Gavilan, H. R.: Analysis of daytime ionosphere behavior between 2004 and 2008 in Antarctica, J. Atmos. Solar-Terrestrial Phys., 73(16), 2272–2278, https://dx.doi.org/10.1016/j.jastp.2011.06.008, 2011.

Correia, E., Raulin, J. P., Kaufmann, P., Bertoni, F. C., and Quevedo, M.T.: Inter-hemispheric analysis of daytime low ionosphere behavior from 2007 to 2011 J. Atmos. Solar-Terrestrial Phys, 92, 51-58, https://doi.org/10.1016/j.jastp.2012.09.006, 2013.

Ern, M., Preusse, P., Gille, J. C., Hepplewhite, C. L., Mlynczak, M. G., Russell III, J. M., and Riese, M.: Implications for atmospheric dynamics derived from global observations of gravity wave momentum flux in stratosphere and mesosphere, J. Geophys. Res., 116, D19107, https://doi.org/10.1029/2011JD015821, 2011.

Fritts, D. C. and Vincent, R.A.: Mesospheric momentum flux studies at Adelaid, Australia: Observations and a gravity wave-tidal interaction model, Journal of Atmospheric Sciences, 44(3), 605-619, https://doi.org/10.1175/1520-0469(1987)044<0605:MMFSAA>2.0.CO;2, 1987

https://doi.org/10.5194/angeo-2019-123
Preprint. Discussion started: 27 August 2019

Fritts, D. C. and Alexander, M. J.: Gravity wave dynamics and effects in the middle atmosphere, Rev. Geophys., 41, 1003, https://doi.org/10.1029/2001RG000106, 2003.

Giongo, G. A., Bageston, J. V., Batista, P. P., Wrasse, C. M., Bittencourt, G. D., Paulino, I., Paes Leme, N. M., Fritts, D. C., Janches, D., Hocking, W., and Schuch, N. J.: Mesospheric front observations by the OH airglow imager carried out at Ferraz Station on King George Island, Antarctic Peninsula, in 2011, Ann. Geophys., 36, 253–264, https://doi.org/10.5194/angeo-36-253-2018, 2018.

Hozumi, Y., Saito, A., Sakanoi, T., Yamazaki, A., and Hosokawa, K.: Mesospheric bores at southern midlatitudes observed by ISS-IMAP/VISI: a first report of an undulating wave front, Atmos. Chem. Phys., 18, 16399–16407, https://doi.org/10.5194/acp-18-16399-2018, 2018.

Jarvis, M. J., Hibbins, R. E., Taylor, M. J., and Rosenberg, T. J.: Utilizing riometry to observe gravity waves in the sunlit mesosphere, Geophys. Res. Lett., 30(19), 1979, https://doi.org/10.1029/2003GL017885, 2003.

Liu, Y., Liang, X.S., and Weisberg, R.H.: Rectification of the bias in the wavelet power spectrum, Journal of Atmospheric and Oceanic Technology, 24(12), 2093-2102, https://doi.org/10.1175/2007JTECHO511.1, 2007

Marshall, R. A., and Snively, J. B.: Very low frequency subionospheric remote sensing of thunderstorm-driven acoustic waves in the lower ionosphere, J. Geophys. Res. Atmos., 119, 5037–5045, https://doi.org/10.1002/2014JD021594, 2014.

Moffat-Griffin, T., Hibbins, R. E., Nielsen, K., Jarvis, M.J., and Taylor, M.J.: Observing mesospheric gravity waves with an imaging riometer, J. Atmos. Sol. Terr. Phys., https://doi.org/10.1016/j.jastp.2008.04.009, 2008.

Nielsen, K., Taylor, M. J., Stockwell, R., and Jarvis, M.: An unusual mesospheric bore event observed at hight latitudes over Antarctica, Geophys. Res. Lett., 33, L07803, https://doi.org/10.1029/2005GL025649, 2006.

Nina, A. and Čadež, V. M.: Detection of acoustic-gravity waves in lower ionosphere by VLF radio waves, Geophys. Res. Lett., 40, 4803–4807, https://doi.org/10.1002/grl.50931, 2013.

Pal, S., Chakraborty, S., and Chakrabarti, S. K.: On the use of Very Low Frequency transmitter data for remote sensing of atmospheric gravity and planetary waves, Adv. Sp. Res., 55(4), 1190–1198, https://doi.org/10.1016/j.asr.2014.11.023, 2015.

Pautet, P.-D., Taylor, M. J., Snively, J. B., and Solorio, C.: Unexpected occurrence of mesospheric frontal gravity wave events over South Pole (90°S), J. Geophys. Res., 123, 160–173, https://doi.org/10.1002/2017JD027046, 2018.

Rozhnoi, A., Solovieva, M., Levin, B., Hayakawa, M., and Fedun, V.: Meteorological effects in the lower ionosphere as based on VLF/LF signal observations, Nat. Hazards Earth Syst. Sci., 14, 2671–2679, https://doi.org/10.5194/nhess-14-2671-2014, 2014.

Sato, K., Watanabe, S., Kawatani, Y., Amd, K., Miyazaki, Y. T., and Takahashi, M.: On the origins of mesospheric gravity waves, Geophys. Res. Lett., 36, L19801, https://doi.org/10.1029/2009GL039908, 2009.

https://doi.org/10.5194/angeo-2019-123
Preprint. Discussion started: 27 August 2019

Scherrer, D., Cohen, M., Hoeksema, T., Inan, U., Mitchell, R., and Scherrer, P.: Distributing space weather monitoring instruments and educational materials worldwide for IHY2007: the AWESOME and SID project. Adv. Space Res., 42(11), 1777–1785, https://doi.org/10.1016/j.asr.2007.12.013, 2008.

Schoeberl, M. R.: Stratospheric warmings: Observations and theory, Rev. Geophys. Space Phys., 16 (4), 521–538, https://doi.org/10.1029/RG016i004p00521, 1978.

Schmitter, E. D.: Data analysis of low frequency transmitter signals received at a midlatitude site with regard to planetary wave activity, Adv. Radio Sci., 10, 279–284, https://doi.org/10.5194/ars-10-279-2012, 2012.

Taylor, M. J. and Garcia, F. J.: A two-dimensional spectral analysis of short period gravity waves imaged in the OI(557.7 nm) and near infrared OH nightglow emissions over Arecibo, Puerto Rico, Geophys. Res. Lett., 22, 2473–2476, https://doi.org/10.1029/95GL02491, 1995.

Torrence, C. and Compo, G. P.: A practical guide to wavelet analysis, Bull. Amer. Meteor. Soc., 79, 61–78, 1998.

Vincent, R.A.: The dynamics of the mesosphere and lower thermosphere: a brief review, Progress in Earth and Planetary Science, 2:4, https://doi.org/10.1186/s40645-015-0035-8, 2015.

Wait, J. R. and Spies, K. P.: Characteristics of the Earth-ionosphere waveguide for VLF radio waves, US Dept. of Commerce, National Bureau of Standards, 1964.

Wang, L., Geller, M. A., and Alexander, M. J.: Spatial and temporal variations of gravity wave parameters. Part I: intrinsic frequency, wavelength, and vertical propagation direction, J. Atmos. Sci., 62, 125–142, https://doi.org/10.1175/JAS-3364.1, 2005.

Zhang, Y., Xiong, J., Liu, L., and Wan, W.: A global morphology of gravity wave activity in the stratosphere revealed by the 8-year SABER/TIMED data, J. Geophys. Res., 117, 21101, https://doi.org/10.1029/2012jd017676, 2012.

https://doi.org/10.5194/angeo-2019-123
Preprint. Discussion started: 27 August 2019

Annales Geophysicae Discussions

Figure Captions

Figure 1: VLF propagation paths from NAA and NPM transmitters to the receiver stations located at Comandante Ferraz Brazilian Antarctic Station (EACF) (blue paths) and Atibaia, São Paulo (red path).

Figure 2: Processed all-sky images of the GW event observed at EACF at three times separated by 10 min on the night of 9-10 July 2007 showing the mesospheric front propagating from southwest to northeast. The first row shows the images with the star field subtracted and applying the Time Difference (TD) image processing, and at the second row are the same images after correcting for the fish-eye lens format. (from Bageston et al., 2011).

Figure 3: VLF amplitude from NAA transmitter station detected with 15 seconds time resolution at EACF on July 10, 2007. The vertical lines mark the sunrise (SR) and sunset (SS) at NAA transmitter station (T, full lines) and at receiver station (R, dashed lines). The periods of completely night and day in the NAA-EACF VLF path are identified. The box marks the time interval of data used to perform the spectral analysis.

Figure 4: Example of wavelet spectral analysis applied to the VLF amplitude signal in the NAA-EACF GCP on 10 June 2007. (a) The residual VLF amplitude after subtracting the raw data from a10-min running mean. (b) Wavelet power spectra in logarithm (base 2), with regions of confidence levels greater than 95% (showed with black contours), and the cross-hatched areas indicating the regions where edge effects become important. (c) time-averaged wavelet power spectra (Global WS). (d) scale-averaged wavelet power.

Figure 5: Same as Figure 4, but for the VLF signal propagating in the NAA-Atibaia VLF GCP.

Figure 6: Monthly gravity wave activity at EACF as detected in the low ionosphere using VLF technique during 2007. The dark blue narrow bar shows the number of the observed days per month, and the colored bars show the number of nights per month with GW events observed according to the GWs predominant periods. The bar colors give the number of waves with predominant period observed in each month separated as the following period intervals: 5 to 10 min (blue), 10 to 15 min (green), 15 to 25 min (purple), 25 to 35 min (orange) and above 35 min (red).

Figure 7: Histogram plot of the predominant observed wave period of the GWs detected in the low ionosphere as amplitude variations of the VLF signal propagating in the NAA-EACF GCP.